ELSEVIER

Polymer 40 (1999) 2981–2991

polymer

Gas induced damage in poly(vinylidene fluoride) exposed to decompression

O. Lorge[a], B.J. Briscoe[a,*], P. Dang[b]

[a]*Department of Chemical Engineering, Imperial College, London SW7 2BY, UK*
[b]*CERDATO, Elf-Atochem, 27470 Serquigny, France*

Received 2 February 1998; revised 29 June 1998; accepted 30 June 1998

Abstract

This paper will discuss the nature of the gas induced damage in a poly(vinylidene fluoride) (PVDF) exposed to 'explosive' or rapid pneumatic decompression in a carbon dioxide environment. Generally, under high pressure, the polymer absorbs significant amounts of gas. The large quantity of gas absorbed may induce a dilatation of the specimen and also influence the mechanical properties of the polymer. When the ambient pressure is reduced, the polymer will often suffer irreversible mechanical damage; this process is usually termed explosure decompression failure or 'XDF'. This paper is presented in four parts. The first part will describe the variation of the mass of the PVDF polymeric sample in a carbon dioxide medium during the compression and the decompression process at 80°C in the pressure range of 0.1–30 MPa. It is shown that the mass of the specimen increases as the pressure increases but, upon decompression under the conditions described, it is quite constant until 15 MPa and then it falls rapidly. The second part describes the corresponding volumetric change of the polymer, in situ, during the compression and the decompression at 80°C. The decompression curve exhibits a dilatation peak centred at around 14 MPa. The decrease of the mass and the size of the sample is related to the generation of cracks in the polymer matrix during decompression. The third part will describe the results of a mechanical deformation experiment on samples exposed to compression–decompression cycles which is used to establish a relationship between the loss of mechanical properties of the sample and the loss of internal coherence due to the presence of internal cracks. A final part summarises the major conclusions which indicate conclusively that the polymer is irreversibly damaged in the decompression process adopted in the current study.

Keywords: Carbon dioxide; Cracks; Explosive

1. Introduction

A major problem with using polymers in a high pressure environment is that they usually display shortcomings in their mechanical endurance when exposed to gases at high fluctuating ambient pressures. Some gases, like carbon dioxide, become a strong solvent for the polymer at high pressure and induced significant dilatation. The effects of this generic solvent sorption property can be very damaging to the polymers. First, the polymer can swell. This is particularly the case for elastomers. Also, the solvent can diffuse into the polymer when in a high pressure environment, so that when the pressure is released the trapped gas tends to nucleate and expand which inflates the polymer matrix thus causing considerable mechanical damage: this is the so-called explosive decompression failure process, 'XFD'. That is the development of a gross internal and surface rupture of the polymer.

Most of the reported studies regarding polymer behaviour during decompression have been conducted on elastomers because of their wide applications in seals and hoses. Two main experimental approaches have been used. One is the measurement of the dilatation of these polymeric samples during decompression. The other is the measurement of physical properties, such as the volume and the Young's modulus, before and after decompression. Moreover, there are different kinds of damage which can occur in the polymer matrix after decompression, such as the growth of bubbles and cracks; it is also possible, under some circumstances, to study these phenomena with optical probes.

The change in the size of a polymeric sample has been measured during decompression with an ultrasonic transducer [1] or with a LVDT [2]. During decompression, the sample size grows with a continuous growth rate until a

* Corresponding author.

0032-3861/99/$ - see front matter
PII: S0032-3861(98)00527-8

sudden increase appears which is an indicator of the growth and propagation of bubbles or cracks inside the elastomeric matrix [2]. Some polymeric specimens, like PTFE or nitrile rubbers, do not appear to expand significantly during decompression [1,3]. However, these authors did not assess if these samples were irreversibly damaged. Zakaria used an acoustic emission technique for the detection of the gas induced cracks [4]. He showed that bubbles appeared around 10 MPa during the particular decompression process adopted.

Many studies have been conducted to determine the size and the mechanical properties of polymers after their environmental decompression. These experiments were carried out normally 10 min after the decompression process. Shade measured the induced post decompression dilatation using the Archimede force [5] method. The change of the Young's modulus, following decompression, very much depends upon the polymer. Zakaria found a decrease in the modulus [6] but Heineck found an increase [7]. A decrease in the elastic limit and of the rupture point have also been observed after decompression experiments [8–10].

The nature of the gas induced damage can also be determined by visual observations [5]. Briscoe and Zakaria sectioned the polymeric samples for subsequent microscopic analysis and detected the cracks produced [6].

Several authors have spoken about bubble nucleation and formation in elastomers [11–16]. Bubbles are produced close to the surface [17–18] and also within the centre of the samples [12]. Hertz also showed that bubble formation characterises the behaviour of elastomers with a few reticulation points, which supports some of the important deformation modes described by Hertz [19].

Cracks have been observed in high-reticuled elastomers [20]. Hertz proposed that the fissures appeared in elastomers with many cross-linked points and supposed that this was caused by the limited extent of their deformation prior to rupture [19]. Usually, the fissures did not appear to reach the surface of the sample [21] and were preferentially oriented. In parallel-piped samples, fissures start in the centre and are parallel to the long side [12]. With cylindrical samples, Liatsis found that the fissures were generally parallel to the major cylinder axis [13].

The present paper examines the gas induced rupture phenomenon of a poly(vinylidene fluoride) (PVDF) polymer in a carbon dioxide environment drawing upon the precedents developed from the previous studies of elastomeric systems. In situ mass sorption and dilatation probes are used in conjunction with post high pressure gas exposure mechanical testing to identify the extent and nature of gas induced mechanical damage for this system.

2. Material and experimental methods

2.1. Material

The poly(vinylidene fluoride) used in this study was PVDF 50 HD (Elf-Atochem, France). Two types of sample were used; rods made from an extruded cylinder, and parallel-pipeds made from an injected sheet. The carbon dioxide gas used was of 99.9% purity (BOC, UK).

2.2. High pressure equipment

The high pressure equipment consisted of a compressed air-driven reciprocating gas pump (Charles Madan, Altrincham, UK) capable of producing a pressure of up to 60 MPa from a gas bottle at ca. 6 MPa (compression ratio of 85:1) (Fig. 1). An intermediate gas receiver, between the pressure vessel and the compressor, permits the damping of any fluctuations in the pressure during pressurisation. The pressure vessel used was 610 mm long with an o.d. of 127 mm and i.d. of 50.8 mm. The gas pressure was released manually through a 3-mm needle valve (up to 6 MPa/min). A detailed description of this assembly has been given elsewhere [22].

The sorption and desorption measurements have been carried out in the pressure range of 0.1–30 MPa, primarily at 80°C. Both mass and volumetric measurements are to be reported.

The experimental procedure adopted was the same for all the experiments described in the subsequent paragraphs. At first, during the compression process, the pressure was increased stepwise (normally in 3 MPa increments) up to 30 MPa. The experimental data were measured every minute for a period of 40 min at each step. Some measurements were undertaken until the equilibrium was supposed to be reached. The criterion to evaluate the condition of equilibrium was the stability of the data, within the experimental precision of the mass or linear dimension, during a period of ca. 20 min.

The decompression measurement procedure was as follows. The pressure was decreased relatively slowly (ca. 0.5 MPa/min) between each step of pressure. When the required pressure value of the step was reached, the mass and the linear expansion of the sample was measured immediately. The next stage of the decompression was then immediately instituted. Adiabatic cooling effects were minimal: less than 5°C at each step.

2.3. Gas mass sorption probe

This experiment allows for the measurement of the increase in the mass of a polymeric sample due to the gas sorption under high pressure. The vibrating beam technique, developed by Briscoe and Mahgerefteh (1984) and later modified and improved by Liatsis (1989) and Zakaria (1990) was used in this study to measure the gaseous mass uptake. The vibrating beam was excited and driven into resonance by an electromagnetic coil. A strain gauge was bonded onto the beam and the frequency and the amplitude and frequency of its vibrations could, thus, be monitored (Fig. 2).

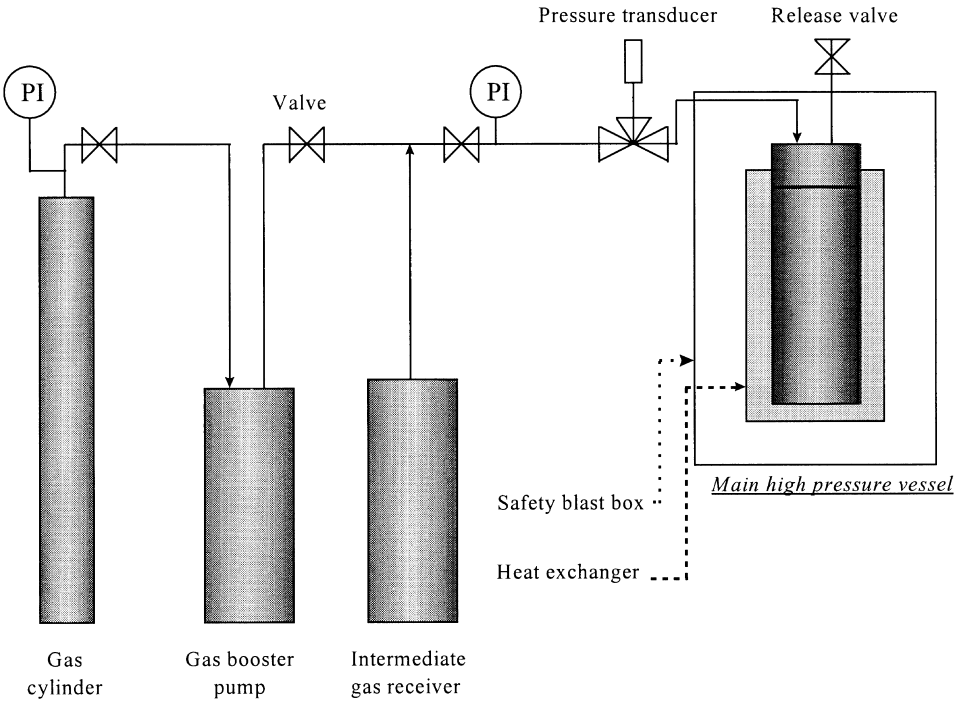

Fig. 1. Schematic layout of the high pressure equipment arrangement.

The technique measures the first harmonic resonant frequency of the system (beam and polymer sample). The resonant frequency changes as the mass of the sample varies during sorption and desorption. Monitoring the frequency provides the necessary data for obtaining the sorption or desorption curves, respectively (mass uptake or loss).

Prescott showed that the period of the oscillations of a beam clamped at one end and having a rest mass attached at

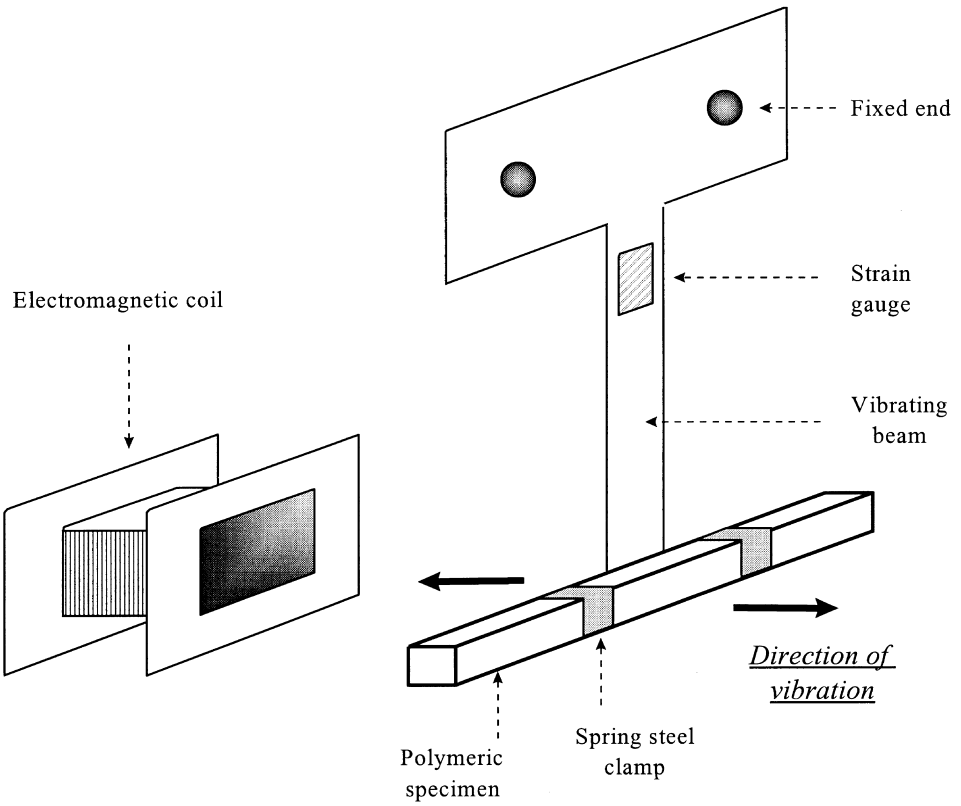

Fig. 2. Mass sorption probe.

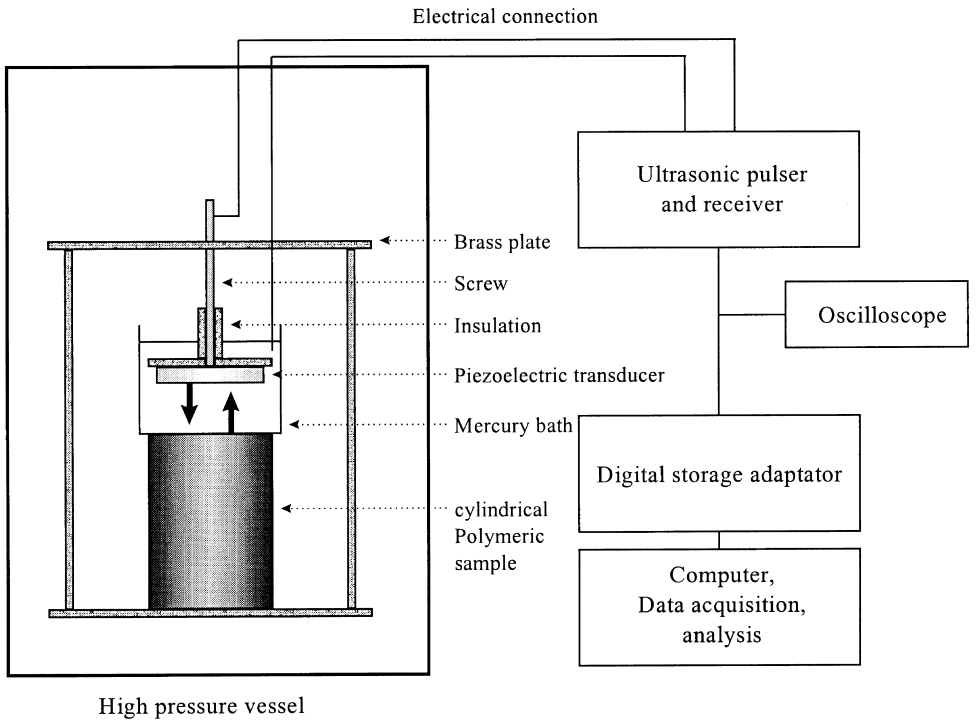

Fig. 3. Schematic representation of the ultrasonic transducer probe arrangement.

the free end is given by the equation [23]:

$$T = \left(\frac{2\pi}{K}\right)\left(\frac{l_r}{x}\right)^2\left(\frac{\rho_r}{E}\right)^{\frac{1}{2}} \quad (1)$$

where T is the period of vibration. K denotes the radius of gyration of the section of the beam about the axis through its centre of gravity perpendicular to the plane of motion. l_r is the beam length, ρ_r is the density of the beam and E the Young's modulus of the beam. The variable satisfies

$$\frac{1+\cosh z\cdot\cos z}{\cosh z\cdot\sin z-\sinh z\cdot\cos z} = cz \quad (2)$$

where c is the ratio of the attached rest mass to the mass of the beam.

So, if c varies, in other words if the rest mass varies, the period of vibration changes. As the other variables remain constant, the period is inversely proportion to the square of the value, as given by

$$\frac{T_0}{T(t)} = \left(\frac{z(t)}{z_0}\right)^2 \quad (3)$$

With the values of $z(t)$, $c(t)$ can be calculated.

In practice a correction must be applied to account for the influence of the entrained gas mass which also induces a frequency change. This correction is obtained by performing a calibration experiment using an inert aluminium specimen of a geometry similar to that of the elastomeric sample. The various frequency measurements were obtained at a fixed vibrational amplitude.

2.4. Dilatation studies

The measurement of the dilatation of the polymeric sample, due to the gas absorbed under high pressure, was carried out using a technique developed by Briscoe et al. and makes use of a single ultrasonic transducer submerged in a mercury bath lying on the top of a cylindrical polymer sample (Fig. 3). This single crystal transducer is used as both a signal transmitter and receiver.

In this method, the time lapsed between the pulse and the echo is measured. The transit time is directly proportional to the path length between the crystal and the top of polymer

$$l_d(t) = v_s\tau(t)/2 \quad (4)$$

where v_s is the velocity of sound in the mercury.

The value of v_s does not depend on the pressure because the mercury is incompressible in this range of pressure. The sound velocity in mercury was taken to be 1441.18 m/s at 42°C [24]. The temperature dependence (dv/dT) of v_s is -0.46 m/s K [25]. The accurate data processing of the electronic signals requires the use of a Fast Fourier Transformation procedure; the details of the method are described elsewhere [3].

2.5. Mechanical apparatus

The damaged polymer specimens were studied in simple diametric (Brazilian type) and axial (upsetting) compression for the cylindrical samples ($D = 20$ mm, $L = 26$ mm) using a commercial mechanical testing machine (Instron 1122, UK) at 20°C. The velocity of the compression was

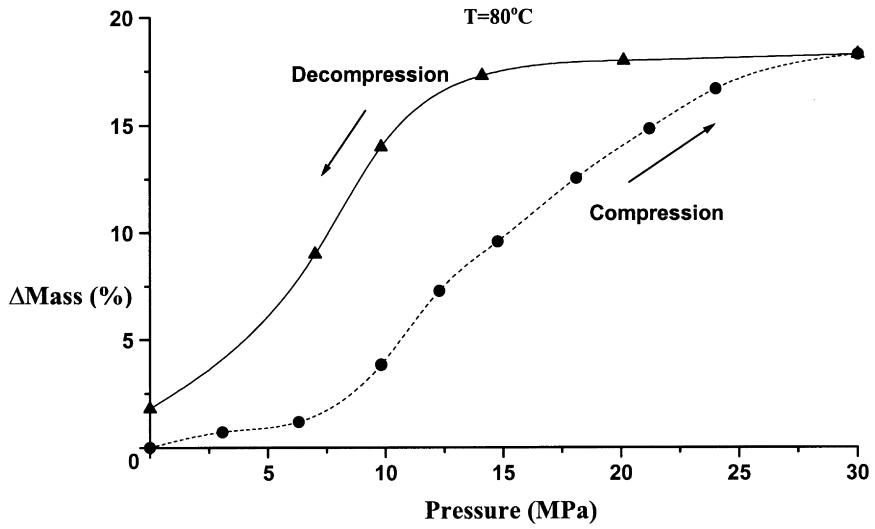

Fig. 4. Mass uptake of the PVDF sample as a function of pressure at 80°C during compression and decompression in CO_2 atmosphere.

0.05 mm/min. No deliberate lubrication was introduced at the polymer/machine interface.

3. Results and discussion

3.1. Gas sorption during compression and decompression

The variation of the mass of the polymeric sample was measured during compression and decompression using the procedures presented previously. The form of the pseudo equilibrium gas compression curve was described in an earlier paper [26]. Essentially, the data were obtained by progressively increasing the pressure in small increments and allowing a period of exposure at each stage to ensure apparent saturation of gas judged by the invariance of the sample mass as a function of time. The decompression measurement procedure was as follows. The pressure was decreased relatively slowly (ca. 0.5 MPa/min) between each incremented step of the pressure decrease. This value was chosen for several reasons. First, it ensured that temperature was reasonably constant; the consequences of the Joule–Thomson effect are significant at rapid decompression rates. Second, it was sufficiently slow to enable the continuous measurement of the mass of the sample. Finally, it was rapid enough to consider the decompression process as being a 'brutal decompression'. When the pressure value of the step was reached, the mass of the sample was measured. This procedure was adopted in order to attempt to mirror as closely as possible the extreme conditions sometimes found during practical explosive decompressions. Typical experimental data are plotted in Fig. 4.

The gas compression curve corresponds to data obtained at near equilibrium adsorption. The shape is typical of the sorption of carbon dioxide in polymers in this temperature range. The desorption curve, which is not the equilibrium case, is seen to lie above the sorption curve but it has a similar form.

Between 30 and 15 MPa, no massive desorption can be identified. The mass of the polymeric sample is quite constant. Several reasons may be proposed in order to explain this situation. First, the diffusion coefficient of the carbon dioxide depends upon the gas concentration. So, the desorption of the sample surface (lower concentration, so lower diffusion coefficient) slows the diffusion process. The second reason was proposed by Crank and is based upon the idea of the formation of a modified surface layer at the surface of the polymer [27]. In this layer, the solvent, i.e. carbon dioxide, has commenced its plasticisation, thus accomodating the swollen polymer chains into the solvent. The more dilute surface layer pushes in the direction of the solvent stream when the gas is sorpted. This process is then reversed when the pressure is released, and thus slows the diffusion process. Finally, and perhaps of more importance, the decompression time at this stage (around 10 min) is rapid enough to avoid an extensive gas desorption.

After 10 MPa, the mass of the sample falls quite rapidly and at a rate which is comparable to that of the sorption curve. This may be due to the development of cracks in the polymeric matrix which permit the flow of carbon dioxide out of the sample. Briscoe and Zakaria reported that cracks appeared after 10 MPa for a silicone elastomer under similar conditions [28]. We may also note that after the complete removed of the ambient pressure (1 bar) some of the gas remains.

3.2. Dilatation during decompression

The variation of the axial linear elongation of the cylindrical polymeric sample was measured during decompression. The decompression measurement procedure was the same as the one explained in the last paragraph. Typical data curves are shown in Fig. 5.

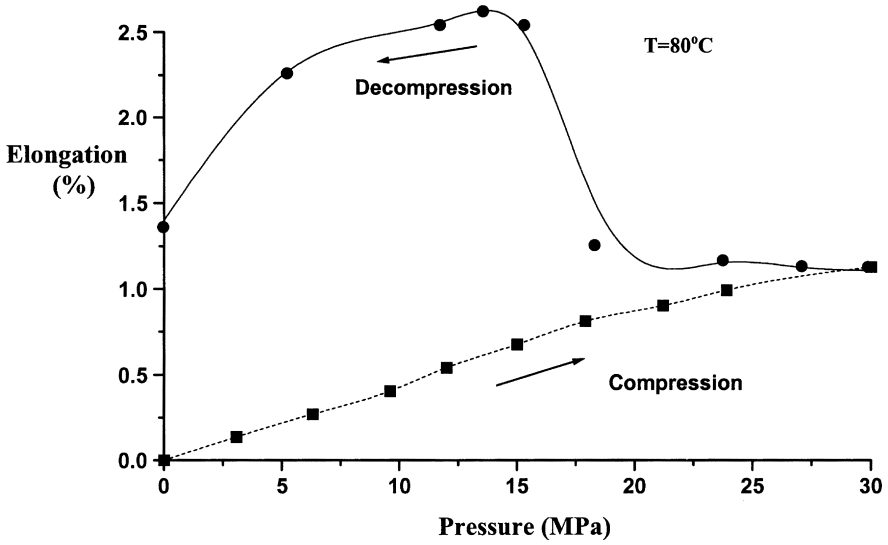

Fig. 5. Linear elongation of the PVDF sample in CO_2 atmosphere as a function of pressure during compression and decompression.

The compression data, which again correspond to a near equilibrium state, show an approximately linear interrelationship between the gas pressure and the linear dilatation. The extent of the expansion does, however, show a detectable decrease in its rate as the pressure is increased. The decompression data, which like the mass sorption data are not near equilibrium, present a peak centred around 10 MPa. Between 30 and 17 MPa, the linear expansion is rather small (a few percent) above the equilibrium values. But around 13 MPa, the dilatation is very significant until the maximum of the peak (ca. 13 MPa). After this point, as is shown in Fig. 4, internal cracks probably appear and a progressive decrease of the linear elongation is noticed as the gas desorbs.

The magnitude of the dilatation peak noted during decompression is directly related to the rate of decompression. The more rapidly the cell is decompressed, the greater is the extent of the maximum dilatation. At a given time, the pressure difference between the interior of the polymer and the ambient will be higher in the rapid decompression case, increasing the dilatatory action of the interior gas upon the polymer matrix. In addition, like the mass sorption data, the sample does not recover its original condition after the compression–decompression process; a permanent inflation is observed which remains for a period of several days.

3.3. Mechanical properties of damaged PVDF

Because PVDF is not transparent, it is not possible to effectively quantify the damage directly by using a direct optical experiment and an alternative approach is to study the consequences upon the mechanical properties. A number of mechanical methods have been used to quantify the extent of the overall gas induced damage produced in polymers. Those used in this study were nominal uniaxial mechanical compression experiments to quantify the decrease in the Young's modulus as induced by the gas decompression.

3.3.1. Uniaxial compression experiment

Damage is not directly accessible to measurement in this polycrystalline system; acoustic and optical probes are not effective. Its quantitative evolution may, however, be linked to the definition of the variable chosen to represent the phenomenon. The definition chosen here is based on the concept of an effective stress.

The introduction of a characteristic damage variable, which represents a surface density of the discontinuities in the material, leads directly to the notion of an 'effective' or sustainable stress; i.e. to the stress calculated over the geometric material section which effectively resists the imposed force. In one loading direction, in the presence of a damage increment D, the effective area of resistance is

$$\tilde{S} = S - S_D = S(1 - D) \tag{5}$$

where S is the total deformed area of the polymeric sample, and S_D is the total area of defect traces present as cracks and cavities. The definition of the effective stress, $\tilde{\sigma}$, is taken here to be

$$\tilde{\sigma} = \sigma \frac{S}{\tilde{S}} \text{ or } \tilde{\sigma} = \frac{\sigma}{1 - D} = E\varepsilon_e \tag{6}$$

where ε_e is the elastic strain and E is the 'intrinsic' Young's modulus, i.e. the elasticity modulus of the material free from any damage. $E(1 - D) = \tilde{E}$ can then be interpreted as the 'effective' elastic modulus of the damaged material. If the coherent or intrinsic Young's modulus is known, a measurement of the elastic stiffness can then be use to determine, and more importantly quantify, the extent of the damage. So, $D = 1 - \sigma/(E\varepsilon_e)$ and with $\sigma = \tilde{E}\varepsilon_e$

$$D = 1 - \frac{\tilde{E}}{E} \tag{7}$$

After an explosive decompression, Briscoe and Liatsis [11] found that for a cylindrical sample of an unfilled elastomer, the cracks were generally concentric, circumferential and

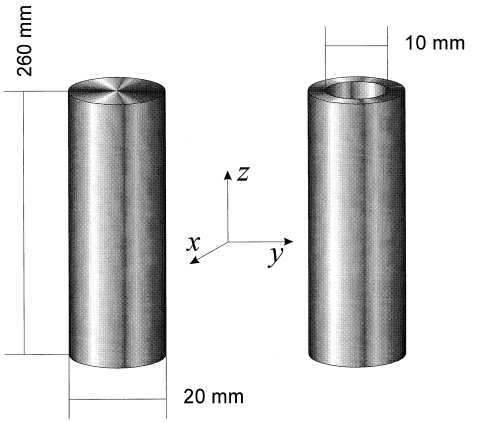

Fig. 6. Schematic views of the tested samples.

parallel to the cylindrical axis (*z*-axis in Fig. 6) of the specimen. There is thus the prospect that mechanical testing of cylindrical samples, in different loading directions, may not only characterise the extent of the internal damage but also identify the orientation and density distribution of the damage. This prospect is examined later.

A range of compression tests (Fig. 6) were undertaken on cylindrical samples ($L = 26$ mm, $D = 20$ mm) after an explosive decompression event or sequence of events. There were no apparent signs of cracks as judged from the inspection of the exterior. Some loss in the mechanical properties are expected such as a decrease in the apparent Young's modulus due to the presence of cracks. The first test style adopted was an axial plain compression (*z* direction in Fig. 6); the data are shown as stress (force normalised by initial compression area of the specimen) as a function of the imposed displacement. The second test style was a diametric compression (*x* direction in Fig. 6). The data are shown for this curve as the load normalised by the length of the rod as a function of the imposed displacement.

Several compression–explosive decompression cycles at 80°C were carried out on cylindrical samples. After each compression, a delay of 5 h was chosen in order to reach the maximum saturation rate. After each decompression, over 1 week was necessary in order to allow most of the trapped gas to diffuse out of the sample. Fig. 7 shows the results of the uniaxial compression tests (axial compression, *z*-axis loading between parallel plates in Fig. 6) as a function of the number of cycles undertaken on the cylindrical samples.

Fig. 7 describes an evolution of the axial compressive stress–displacement curves of several PVDF samples with the number of gas induced compression–decompression cycles. The calculated value of the Young's modulus (proportional to the slope of the curves of Fig. 7 in the range of displacement of 0.2–0.8 mm) decreases with the increase in the number of pneumatic cycles. Using Eq. (7), it is now possible to provide a quantitative estimation of the damage evolution as a function of the number of cycles. After one cycle, a value of of 3.5% is found. This value establishes the presence of defects introduced by the decompression process. In Fig. 9, the results obtained for the computation of the damage parameter for the higher number of decompression cycles are given.

Further mechanical tests were carried out on the cylindrical samples but this time, they were lying horizontally to the imposed force (diametric compression, the *x*–*y* plane in Fig. 6). The experimental curves, showing the load normalised by the length of the rod as a function of the displacement, are shown in Fig. 8 as a function of the number of gas decompression cycles.

The values of these curves do not depend of the direction of the load in the *x*–*y* plane. This means that the damage is uniformly distributed along this plane. In the linear part of the curves, the derivative of the load with respect of the strain, decreases with the number of compression–decompression cycles. Considering that the decrease is

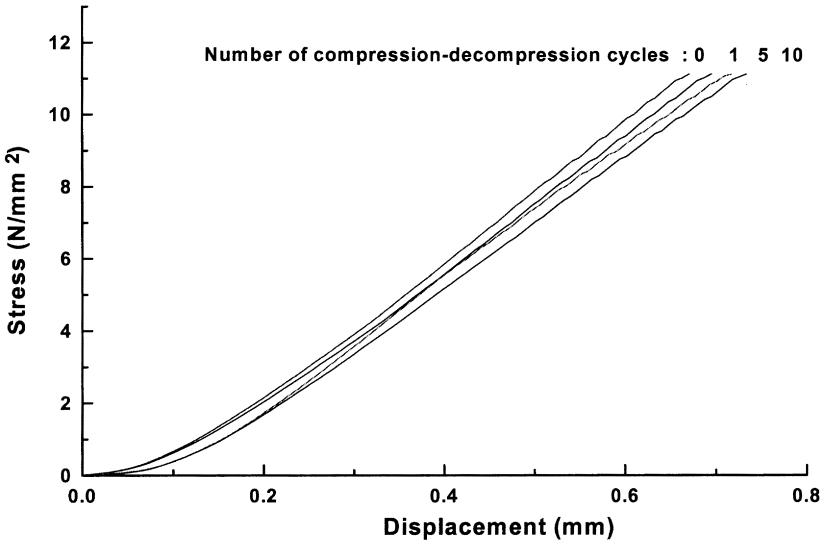

Fig. 7. Stress–displacement curves of PVDF samples for axial compression (*z*-axis loading in Fig. 6) after several compression–decompression cycles at 80°C.

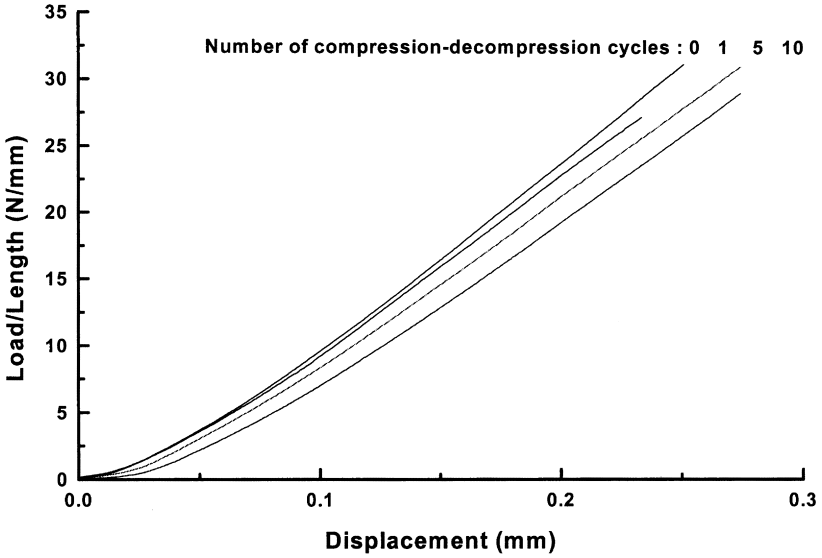

Fig. 8. Load (normalised by the length of the rode)–displacement curves of PVDF samples in the Brazilian configuration (diametric compression, the x–y plane in Fig. 6) after several compression–decompression cycles at 80°C.

due to the formation of cracks in the polymer, and using the derivative instead of the Young's modulus in Eq. (7), a value of the damage parameter was computed and is showed in Fig. 9 along with the corresponding data obtained from Fig. 7.

In Fig. 9, which shows the computed damage parameter (calculated using Eq. (7)), it appears that the two kinds of tests (axial and diametric compressions) provide the same type of information. Initially, the majority of the sensed mechanical damage appears during the first compression–decompression cycles (for the axial case and for the diametric configuration). Then, the evolution of is slow and reaches, after 10 cycles, values of 6.5 and 9% for the axial and diametric compressions, respectively. These values also show that the polymer does not physically explode after a large number of cycles. However, the presence of cracks in the polymer matrix which deteriorate the mechanical properties, can induce premature failure problems during their use.

Shieh et al. [30] have also reported a loss in the mechanical properties after decompression for many polymers. They performed tension tests on polymers submitted to carbon dioxide atmosphere (at 20 MPa) for 1 h and decompressed in 1 h at 70°C. The tests were carried out at 23°C. The computed damage parameters found were 8.9% for polypropylene, 5.4% for poly(oxymethylene), 18.8% for low-density polyethylene and 3.8% for high-density polyethylene. Nevertheless, an increase in the mechanical properties was found for Nylon 66 (an increase of 2.3% of the modulus of elasticity).

The localisation or relative positions and extents of the defects is of interest in order to understand what was occurring during a decompression event. Briscoe and Liatsis have also observed circular cracks near the surface in their work

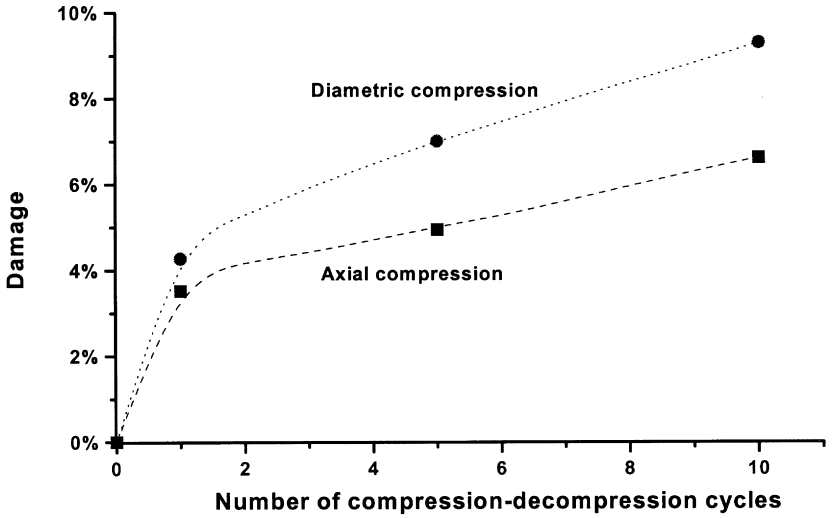

Fig. 9. Evolution of the damage in function of the number of compression–decompression cycles.

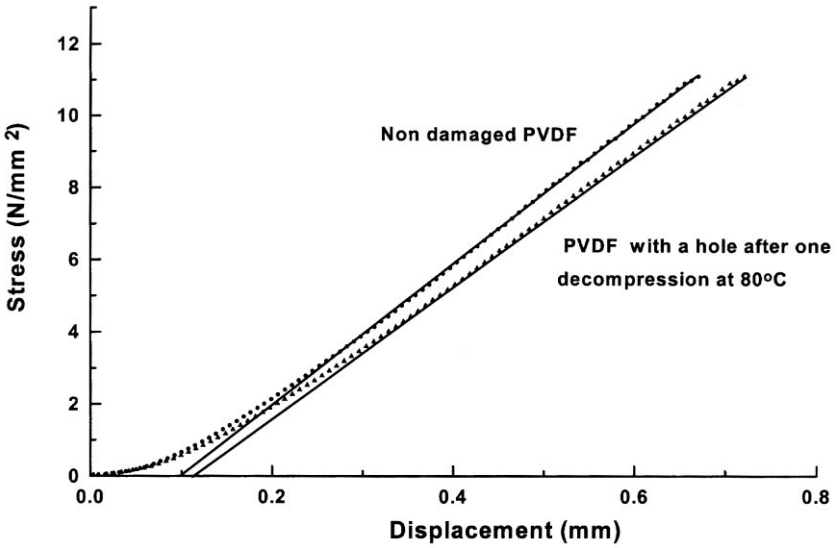

Fig. 10. Stress–displacement curves of two PVDF samples with an axial hole obtained by axial compression. One is a non-damaged polymer and the other one was tested after an explosive decompression under carbon dioxide atmosphere at 80°C.

on the explosive decompression of commercial seals [13]. In order to examine if the same phenomena occurs in PVDF, one more compression experiment was carried out. An axial hole of 10 mm was made in the cylindrical samples after the compression–decompression experiment was done, as is shown in Fig. 6. The axial compression test was also carried out on a non-damaged cylinder with a 10-mm hole. In Fig. 10, the results of these two axial compression experiments are given as the real stress as a function of the displacement. Using these two experiments, the damage parameter of the periphery of the cylinder can be computed. This value of the damage can be compared to the one of the overall cylinder. If the $D_{\text{periphery}}$ is higher than the D_{overall}, it will mean the defect concentration is higher in the periphery than in the overall cylinder. In contrast, a smaller $D_{\text{periphery}}$ would show that the defect concentration is higher in the inner region.

With the value of the Young's modulus measured from Fig. 10, $D_{\text{periphery}}$ equals 5% instead of 3.5% (D_{overall}) (Fig. 7), expected for an homogeneous distribution of the defects in the polymer.

These two values of D show that the defects are more concentrated in the periphery of the polymer samples and that no significant damage occurs in the central regions.

It would be attractive to suppose that the differences in magnitude of the evolution of the mechanical properties for the two uniaxial deformation configurations could be used to further identify the internal geometry of the cracks and fissures. Intuitively, one might have supposed that if the cracks had a propensity to form in circumferential configurations, as had been proposed, then the rate of change of with the number of gas decompression cycles would have been sensed more extensively for the case of the diametric compressions; this is the case, see Fig. 9. The problem is clearly complex and an intuitive explanation must only suppose that a loss of stiffness will occur in both cases. Currently, a numerical simulation of the consequences of various damage site geometries and dispositions is being implemented [29].

A simple comparison can be made just by comparing the mechanical behaviour of the damaged polymeric sample to that of a non-damaged sample with an identical geometry but with an axial hole. This internal hole can induce the same type of mechanical loss as the proposed circumferential fissures in the material as induced by the gas. The data of Fig. 11, show the values of the effective damage due to the presence of the hole (using the derivative of the load as a function of the displacement instead of the Young's modulus in Eq. (7)) as a function of the size of the internal holes (in percent) as a fraction of the real diameter for both radial and axial unidirectional compressions.

In the case of radial compression, a small hole induces a greater value of the damage parameter as compared to the axial deformation. This kind of experiment provides a good indicative test for the presence of circumferential fissures. With the extrapolation of Fig. 11, we can see a damage factor of 9% is reached with an internal hole of 4% of the initial radius. So, mechanically, in the radial direction, the damaged polymeric cylinder reacts as a tube with a hole of 4% of the rod radius.

As is shown in Fig. 11, circumferential fissures are not detected to a high degree of sensitivity by the axial compression deformation (for a damage value of 6.5%, a hole radius of 25% is needed). This kind of experiment would primarily reveal fissures oriented at an angle of 45° with the axis.

The fact that the uniaxial deformation does sense the damage, albeit to a lesser extent than the transverse compression, does suggest that some damage with this type is present and that the orientations are not entirely directed in a cylindrical geometry. Thus, in this sense the mechanical

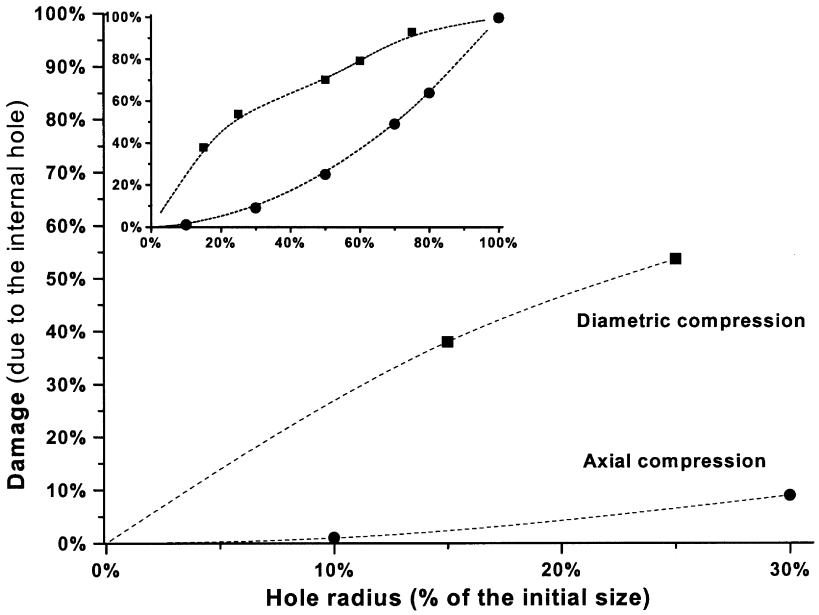

Fig. 11. Damage due to an internal axial hole as a function of the hole radius.

tests do not conclusively reveal the dispositions and orientations of the damage zones.

4. Conclusion

The behaviour of a PVDF during a decompression process in a carbon dioxide atmosphere under high pressure was studied, using experimental techniques for the measurement of gas mass absorbed in the polymer and the corresponding polymer dilatation. The mass desorption and the dilatation isotherms at 80°C in a range of pressure of 0.1–30 MPa were provided.

The mass desorption curve shows a marked decrease after 15 MPa. The expansion of the polymer during the decompression is centred around 14 MPa. These phenomena are probably due to the generation of cracks in the polymer matrix which facilitate the short circuit diffusion of the sorbed gas out of the polymeric matrix.

The generation of cracks in the polymeric matrix was established and quantified using two simple mechanical compression tests: uniaxial axial and diametric compressions. Cracks have been tentatively deduced to be mainly in the periphery of the polymer matrix, as proposed by Briscoe and Liatsis [10]. The various mechanical deformation experiments suggest some preferential orientation of damage sites but the data are generaly inconclusive. The damage was estimated at 3.5% after one compression–decompression cycle and 6.5% after 10 cycles, as sensed by axial loading. The damage sensed is higher for the diametric deformation: 4 and 9%, respectively, under corresponding conditions. The shape of the curve which shows the evolution of the damage as a function of the number of compression–decompression cycles, indicates that the initial decompression cycle caused the majority of the observed disruption and that the extent of the secondary the damage, caused by repeated cycles of compression and decompression, does not increase dramatically with the increase in the number of compression–decompression cycles after the first exposure. As a first order explanation, we may suggest that the damage sites provide short diffusion paths and ‘soften’ the sample in such a way that the decompression rupture stresses are less effective. The fact that the fissures may form effective nucleation sites in subsequent decompression events is apparently of lesser importance.

Acknowledgements

The authors thank Elf Atochem and especially the CERDATO research centre for their help and sponsorship.

References

[1] Briscoe BJ, Zakaria S. J Polym Sci: Phys Ed 1991;29:989.
[2] Ender DH. Chem Techn 1986, 52.
[3] Briscoe BJ, Zakaria S. Polym Testing 1990;9:103.
[4] Briscoe BJ, Zakaria S. In: Proceedings 2nd international conference, ‘Electrical, Optical and Acoustic Properties of Polymers’, 11–12 September 1990.
[5] Shade WN, Legg DW. J Eng Gas Turbines Power 1988;110:289.
[6] Briscoe BJ, Zakaria S. J Material Sci 1990;25:3017.
[7] Heineck DW, Rader CP. 133th Meeting, Dallas, TX, 1988, paper 40.
[8] Kosmala JL, Sohlo AM, Spoo BH. 124th Meeting, Houston, TX, 1983, paper 64.
[9] Potts DJ. PRI Discussion Forum and Exhibition on ‘Offshore Engineering with Elastomers’, Aberdeen, 1985, paper 21.
[10] Shieh YT, Su J-H, Manivannan G, Lee PHC, Sawan SP, Spall WD. J Appl Polym Sci 1996;59:695.
[11] Briscoe BJ, Liatsis D. Rubber Chem Techn 1992;65:350.

[12] Campion RP. Cellular Polymers 1990;9:206.
[13] Liatsis D. PhD thesis, Imperial College, 1989.
[14] Stewart CW. J Polym Sci: Part A-2 1970;8:937.
[15] Gent AN, Tompkins DA. J Appl Phy 1969;40:2520.
[16] Denecour RL, Gent AN. J Polym Sci: Part A-2 1968;6:1853.
[17] Pugh T, Goodson J. Offshore, 1992, 39.
[18] Campion RP. PRI International Conference on 'Polymer in Offshore Engineering', Scotland, 1988, paper 5.
[19] Hertz DL. Machine Design 1981;53:209.
[20] Gent AN, Tompkins DA. J Polym Sci: Part A-2 1969;7:1483.
[21] Cox VA. PRI Discussion Forum and Exhibition on 'Offshore Engineering with Elastomers', Aberdeen, 1985, paper 19.
[22] Briscoe BJ, Mahgerefteh H. Phi Mag 1986;A54:131.
[23] Prescott J. Applied electricity. London: Longman, 1924.
[24] Shih WY. PhD thesis, Imperial College, 1996.
[25] Kaye GWC, Laby TH. Tables of physical and chemical constants. London: Longman, 1986.
[26] Briscoe BJ, Lorge O, Dang P. J Polym Sci: Phys Ed, submitted.
[27] Cranck J, Park GS. Diffusion in polymers. New York: Academic Press, 1968.
[28] Zakaria S. PhD thesis, Imperial College, 1990.
[29] Briscoe BJ, Lorge O. Dang P. Polymer, submitted.
[30] Shieh YT, Su JH, Manivannam G, Lee PHC, Sawan IP, Spall WD. J Appl Polym Sci 1996;59:695.